P-42

INFLUENCE OF CROSS-SECTION MODIFICATION OF PP FIBRES ON THE END-USED PROPERTIES

JOZEF RYBA[a], ANNA UJHELYIOVÁ[a], ĽUBA HORBANOVÁ, and PETER MICHLÍK[b]

[a] Department of Fibres and Textile Chemistry, Institute of Polymer Materials, Faculty of Chemical and Food Technology, Slovak University of Technology in Bratislava, Radlinského 9, 812 37 Bratislava, Slovakia, [b] Research Institute for Man-Made Fibres, a.s., Štúrova 2, 059 21 Svit, Slovakia
jozef.ryba@stuba.sk

Abstract

Shape of cross-section of the fibres has significant influence on end-used properties of fibres which are used for textile or technical applications. This work is focused on an evaluation of the influence of this varied fibre geometry on different properties and characteristics of polypropylene (PP) fibres.

Introduction

Ones of the main end-used properties of textile materials are mechanical and transfer properties (heat, humidity and air).

The transfer properties of fibres correspond mainly with their surface properties. The transfer properties of fibres are mainly related to their geometry. The cross-section and longitudinal fibre geometry is defined by the following characteristics such as shape and size of fibre surface, volume of fibre, measuring surface of fibres and capillary system between the fibres and yarns. A great variety of fibre profiles with different surfaces and sur-face properties can be reached during the technological conditions of synthetic fibre spinning and drawing by profiling in cross-section and longitudinal direction[1-3].

Shaped fibres with special or strongly irregular profiles are very promising. They are manufactured with spinnerets with the appropriate profile of holes[4]. The shaped fibres can be used to develop new kinds of textiles and low-melting knits, since the irregular profile sharply increases the frictional forces between filaments. In addition, the high covering power of the shaped fibres reduces materials consumption for the articles.

For evaluation of shaped fibre characteristics are used following relations:

Degree of branching:	$R=P_N^2/S_N$	
Filling degree:	$Z=S_N/S_Y$	
Degree of segmentation:	$S_e=P_N/P_Y$	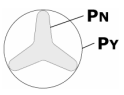
Degree of deformation:	$D=R/r$	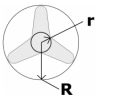
Coefficient of fullness (for hollow fibres):	$F_P=(1-A_D)/A_V$	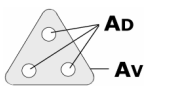

P_N – circumference of cross-section, S_N – surface of cross-section, S_Y – surface of circumscribed circle, P_Y – circumference of circumscribed circle, R – radius of circumscribed circle, r – radius of inscribed circle, A_D – surface of hollows, A_V – surface of fibre

Triangular and three-pronged — "trilobal" — are the most frequently encountered shape. Triangular fibres with a flat surface can be used to manufacture articles with a "luster effect" due to high light reflection by their individual segments. Fibres with a flat (more precisely, oval) section also have a luster effect. In addition, high flexibility is characteristic of these fibres due to the lower moment of inertia of the flat section in flexure in comparison to round sections[4].

This article deals about influence of the cross-section shape of the polypropylene fibres onto above mentioned end-used properties.

Experimental

Materials used

For the preparation of non-modified (nPP) and modified PP (mPP) fibres was used polypropylene Tatren HT 1810 with MFI = 20.9 g/10 min from Slovnaft a.s., Slovakia and micronized inorganic filler (6.4 wt.%). From these materials were prepared undrawn fibres with circle and five pointed star shape cross-section and modified by inorganic filler on the laboratory spinnig machine. Next, the undrawn PP fibres have been to drawn to the drawing ratios $\lambda = 3$ and 4.

Method used

Mechanical properties were measured on INSTRON 1122 and evaluated according to STN EN ISO 1973, 5079, 2062 – standard methods for evaluation of mechanical parameters.

For evaluation of shaped PP fibre characteristics was used optical microscope Olympus BX51 equipped with CCD camera and software analySIS FIVE version 5.0 (build 1120).

For evaluation of water vapour sorption of PP fibres was used gravimetric analysis. Samples were dryed at 80 °C for 1 hour in drying chamber. After that samples were puted into glass vessel with saturate solution of NH_4NO_3 (relative humidity over this solution is 65 % at 20 °C) for 96 hours. After this period the samples were weighing. In the next step samples were dryed in drying chamber at 105 °C for 3 hours and weigh again.

Content of water vapour (C_{WV}) sorption was calculated on the backround of this formula:

$$C_{WV} = \frac{m - m_0}{m_0} * 100\% \qquad (1)$$

were m – weight of the fibre with water vapour sorption in equilibrium state (after 96 hours), m_o – weight of the fibre after drying.

Results

Mechanical properties of non-modified and modified PP fibres are shown in Table I and Table II. Tenacity at the break of PP fibres modified by micronized inorganic filler is lower in comparison with non-modified PP fibres at both drawing ratios λ=3 and 4. This is caused by particle size of micronized inorganic filler, which decrease the sufficiency of drawing of polymer matrix. This type of inorganic filler has no reinforcement effect on PP fibre matrix. However tenacity at the break of non-modified and modified PP fibres with cross-section shape of five pointed star is higher than tenacity at the break of non-modified and modified PP fibres with circle shape cross-section. The micronized inorganic filler due to decrease of tenacity at the break of PP fibres with cross-section shape of five pointer star in comparison with the non-modified PP fibres with the same cross-section shape. This confirms the theoretical knowledge, that the addition of micronized filler to the oriented polymer matrix decreases their mechanical properties. These all statements are analogical for Young's modulus as well as elongation at the break.

Next part of end-used properties of non-modified and modified PP fibres is shown in Tables III and IV. Cross-section area (A) of circle shape cross-section of modified PP fibres is higher in comparison with cross-section area of non-modified PP fibres. This is caused by present of micronized inorganic filler (lower filament diameter homogenity). Cross-section area of the PP fibres with five pointed star cross-section shape is higher than cross-section area of the PP fibres with circle cross-section shape. This can cause the different cooling and crystallization of PP melt flow from various profiles of hole at the same conditions of preparation.

Table I
Fineness (T_d), tenacity (σ) and elongation (ε) at the break, Young's modulus (E) of the non-modified and modified PP fibres with drawing ratio λ=3

Sample	T_d [dtex]	σ [cN/dtex]	ε [%]	E [cN/dtex]
nPP-circle	6,0	2,8	155	24,8
mPP-circle	6,3	2,6	139	23,4
nPP-star	6,0	3,4	158	26,2
mPP-star	6,2	3,0	185	21,8

Table II
Fineness (T_d), tenacity (σ) and elongation (ε) at the break, Young's modulus (E) of the non-modified and modified PP fibres with drawing ratio λ=4

Sample	T_d [dtex]	σ [cN/dtex]	ε [%]	E [cN/dtex]
nPP-circle	6,1	3,4	117	35,3
mPP-circle	6,2	3,0	95	32,5
nPP-star	5,9	4,2	140	35,0
mPP-star	6,4	3,6	122	27,0

Table III
Cross-section area (A), degree of branching (R), filling degree (Z), degree of segmentation (S_e), content of water vapour (C_{WV}) of the non-modified and modified PP fibres with drawing ratio λ=3

Sample	A [μm^2]	R	Z	S_e	C_{WV} (wt.%)
nPP-circle	535	–	–	–	1,05
mPP-circle	670	–	–	–	1,15
nPP-star	604	24,8	0,63	1,09	1,21
mPP-star	940	20,9	0,67	1,05	1,30

Degree of branching (R) and degree of segmentation (S_e) of the non-modified and modified PP fibres with five pointed star cross-section shape decrease with increasing drawing ratio. Filling degree (Z) of the non-modified and modified PP fibres with five pointed star cross-section shape slightly encrease with higher drawing ratio.

All calculated parameters (R, Z, S_e) obtained by optical microscopy for fibres with circle cross-section shape are equal 1.

Table IV
Cross-section area (A), degree of branching (R), filling degree (Z), degree of segmentation (S_e), content of water vapour (C_{WV}) of the non-modified and modified PP fibres with drawing ratio λ=4

Sample	A [μm^2]	R	Z	S_e	C_{WV} (wt.%)
nPP-circle	560	–	–	–	0,61
mPP-circle	705	–	–	–	0,70
nPP-star	630	23,9	0,64	1,11	0,83
mPP-star	811	20,7	0,69	1,06	0,99

Content of water vapour sorption of modified PP fibres is higher than sorption of non-modified PP fibres. This is also caused by present of micronized inorganic filler which can invade surface homogenity of each filament of the fibre. These all statements are analogical for both types of cross-section shape of the fibres and drawing ratios.

The PP fibres with the circle shape cross-section as well as with five pointed star cross-section shape at the lower drawing ratio (λ=3) have higher segmentation of their profile and it provide the higher water vapour sorption of these fibres.

Conclusion

On the backround of experimentally obtained results it can be concluded that:

– change of cross-section geometry from circle to five pointed star have positive influence onto tenacity and Young's modulus of the non-modified and modified PP fibres,

− cross-section area of the fibres with five pointed stars cross-section shape is higher than cross-section area of circle cross-section shape fibres and have positive influence on content of water vapour sorption.

Modificated fibres like these are applicable for technical fabric and for improving of the other types of materials like concrete for example.

This work was supported by the VMSP-P-0007-09 and VEGA 1/0444/09.

REFERENCES

1. Jambrich M.: Fibres Text. East. Eur. *6*, 33 (1998).
2. Murárová A.: Chemical Papers. *47*, 356 (1993).
3. Murárová A.: Chimvolokno *3*, 56 (1993).
4. Perepelkin K. E.: Fibre Chem. *37*, 123 (2005).

P-43
COMPARISON OF INJECTION MOLD COOLING SYSTEMS

STEPAN SANDA, MIROSLAV MANAS, DAVID MANAS, MICHAL STANEK, and JIRI KNOT

Tomas Bata University in Zlín, nám. TGM 5555, 760 01 Zlín, Czech Republic
sanda@ft.utb.cz

Abstract

This article deals with a problem of the injection mold cooling. For the two cavities, injection mold was designed different cooling systems. The first system was made by drilling holes and the second cooling system was made by DMLS technology – rapid prototyping. Both systems were compared with the help of the CAE application.

Introduction

Cooling system of injection mold affects the quality of injected part and cycle time. The most common design of cooling system is in the form of drilled holes or milled channels. Machining of holes and channels is time consuming process and does not enable to set up steady temperature distribution inside the cavity mold. DMLS (Direct Metal Laser Sintering) is one of the Rapid Prototyping technologies that any geometry of cooling system makes possible.

Compared cooling system

Two-plate injection mold with cold runner system and cylindrical ejector pins has been chosen for comparison of conventional and new (generative) cooling systems. Design of the injection mold enables to change cavity only regardless of used cooling system.

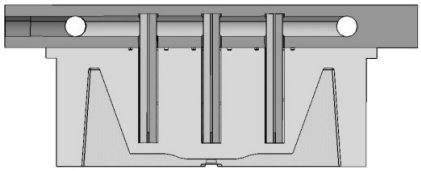

Fig. 1. **Cavity of classical cooling system**

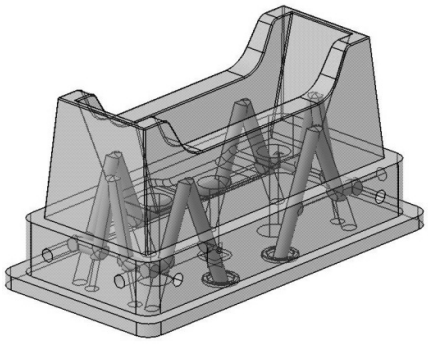

Fig. 2. **Core of classical cooling system**

The first of the cavity has conventional cooling system and another one is made by DMLS technology. The DMLS technology makes possible to create complicated holes with diameter of 4 to 5 millimetres, which more effectively cool down cavity and core.

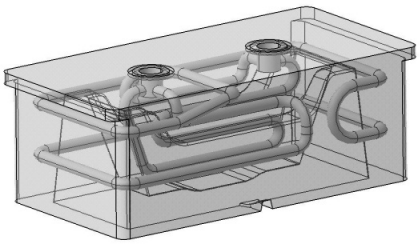

Fig. 3. **Cavity of DMLS cooling system**

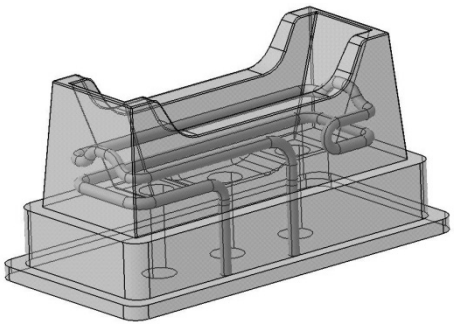

Fig. 4. **Core of DMLS cooling system**

CAE analyses

Comparison of both cooling systems was carried out with Autodesk Moldflow Insight 2010, where were defined cavity, gating and cooling system. The same process condition, 3D volume mesh and same analyses sequence has been used in all analyses.

DMLS technology

Direct Metal Laser Sintering (DMLS) rank among Rapid Prototyping (or Rapid Tooling) technologies. This technology enables production of part with very complicated geometry.

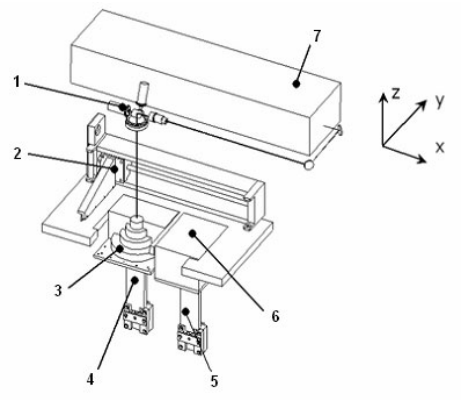

Fig. 5. **Principle of DMLS technology;** 1 – galvanometer-scanner with f-Theta lens; 2 – laminated system; 3 – product of DMLS; 4 – structural platform; 5 – storage bin platform; 6 – storage bin; 7 – laser.

Building of product is realized layer by layer (so called generative method). The laser beam melts metal powder in very thin layer. Suitable materials for DMLS technology are bronze, tool steel, stainless steel, titanium, Co-Cr alloys etc. The product is homogenous metal part with similar properties like the product made by the working.

The advantage of new technology for design of cooling system of injection mold lies in unlimited shapes of cooling channels, generation of turbulent flow coolant and uniform temperature distribution.

Discussion

Results confrontation of both cooling systems show the more uniform temperature distribution by the DMLS products. This fact is very clearly seen in the Fig. 6 and Fig. 7 describing efficiency of heat removal by the given circuit.

This efficiency depends on the shape of the cooling channel, the distance of cooling channel from the cavity wall, Reynolds number and type of coolant. The cooling channels made by the classical way are thermal overloaded inside of cavities. This problem does not appear by the DMLS parts where all parts of cooling systems have been thermal steady loaded.

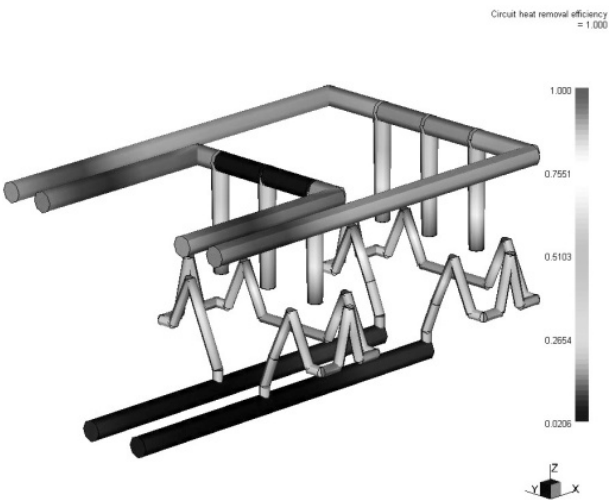

Fig. 6. **Circuit heat removal efficiency of classical cooling system**

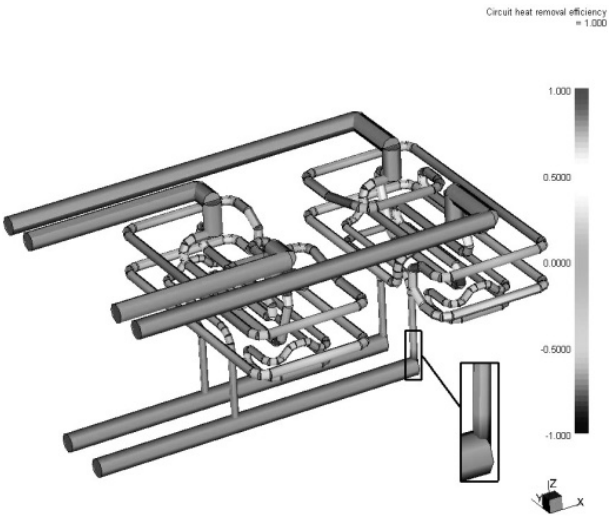

Fig. 7. **Circuit heat removal efficiency of DMLS cooling system**

Thanks to new design of cooling system made by DMLS technology the cycle time was of 10 seconds shorter in comparison with traditional one. Besides this, the dimensional stability of final part has been improvement.

Conclusion

DMLS as new technology in production of metal parts could be an alternative for production of parts with very complicated geometry, which cannot produce by traditional technology. New way in production of cooling systems of injection mold leads to improvement of part quality and reduce significantly cycle time mainly due to steady temperature distribution.

This article is financially supported by the Czech Ministry of Education, Youth and Sports in the R&D projects under the titles 'Modelling and Control of Processing Procedures of Natural and Synthetic Polymers', No. MSM 7088352102 and 'CEBIA Tech', No. CZ.1.05/2.1.00/03.0089.

REFERENCES

1. Knot J.: *Diplomová práce*. Univerzita Tomáše Bati ve Zlíně, Zlín 2010.
2. DMLS [online]. 2007 [cit. 2010-11-01]. DMLS - Direct Metal Laser Sintering, Kovové prototypy. Dostupné z http://www.dmls.cz.
3. Mayer S.: Conformal cooling: Why use it now?. Injection Molding [online]. December 8th, 2009, [cit. 2010-11-01]. Dostupný z http://www.plasticstoday.com/imm/articles/tooling-conformal-cooling-1209.
4. Šanda Š., Maňas M., Staněk M., Maňas D., Rozkošný L.: Chem. Listy *103* (S), 140 (2009).

P-44
CO_2 LASER MICROMACHINING AND PLASTICS PROPERTIES

LIBUŠE SÝKOROVÁ and OLDŘICH ŠUBA

Tomas Bata University in Zlín, Faculty of Technology, Department of Production Engineering, T. G. Masaryka 275, 762 72 Zlín, Czech Republic
sykorova@ft.utb.cz

Introduction

There are several types of plastics that have been processed by laser. They absorb electromagnetic energy at 10.6 micrometers – the wavelength of light emitted by CO_2 lasers.

The task of the laser micro-machining has very extensive usage in industrial applications. Production specifications trend to continual minimization of product's dimensions. The laser is optimal tool for its features in this development. Results of the laser micro-machining – surface quality of product and his utility in specific application – depend on the laser parameters and the polymer material type.

Experiment

From the obtained scientific knowledge it follows, that the character of surface machined by laser depends among others on the thermal conductivity of polymer. Therefore it was decided to test more kinds of polymers – ABS and PMMA. Commercial CO_2 laser Mercury L-30 by firm Laser-Pro, USA was used for cutting of specimens. Ray of laser could be focused on mark diameter d = 185 μm. The maximum value of density of energy flow is q = 1,1 GWm^{-2}.Desired symbol was created in program Corel Draw, the width of slot was 2 mm in all cases. Cutting parameters (output power and feed) were set and these were changed gradually. Values of power and feed are presented as percents from maximum power (P = 30 W) and maximum feed (fmax = 1066 mm s^{-1}) in charts of parameters combination and graphs. These specimens were prepared from this sheet (proportions 130 x 61 mm, thickness 10 mm). The edges were milled and grinded. Dependence of slot depth on the laser parameters – output power and feed – was measured. The dimension and profiles measuring of machined slots were realized on the optical microscope ZEISS 2772. Suitable microscope optics which ensured 117 x enlargements was set first of all. For the reason of statistical evaluation of measured values the measurement of depth was realized in all slots 5 times. Slot depth (d in μm) in dependence on laser parameters combination is presented in following results tables. Values of power and feed are presented as percents from maximum power (P = 30 W) and maximum feed (f_{max} = 1066 mm s^{-1}) in charts of parameters combination and graphs. Description 20/70 means 20 % value from power 30W and 70 % value from maximal feed 1066 mm s^{-1}.

Especially at short power slot values were very short and it was not possible to measure. These experimental results

Table I
Slot depth in μm for ABS

P [%] f [%]	10	20	30	40	50	60	70	80
50	–	10	75	90	105	118	162	206
70	–	–	10	54	68	75	102	127
100	–	–	–	20	31	65	75	101

Table II
Slot depth in μm for PMMA

P [%] f [%]	10	20	30	40	50	60	70	80
50	24	38	102	126	178	200	246	248
70	–	3	15	39	51	116	146	160
100	–	–	8	25	31	37	47	63

Table III
Regression equation of slot depth dependencies on laser parameters combination designated in program EXCEL

Feed f [%]	equation	correlation coeffic. R^2
	PMMA	
50	y = 3,5167x	0,9759
70	y = 2,8929x	0,9525
100	y = 0,9914x	0,9681
ABS		
50	y = 2,8214x	0,9432
70	y = 2,1029x	0,9536
100	y = 2,0600x	0,9735

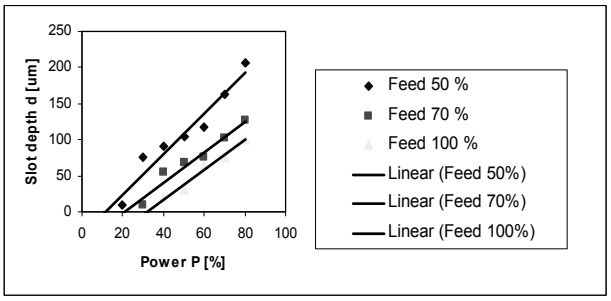

Fig. 1. **Slot depth linear dependence for ABS**

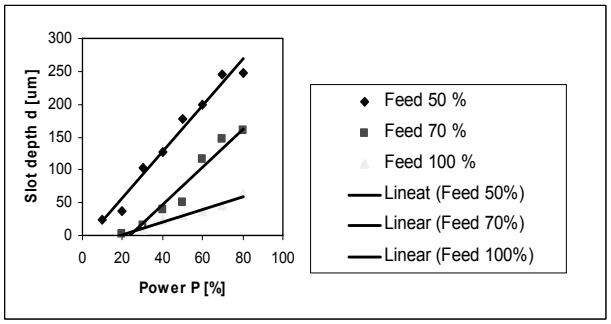

Fig. 2. **Slot depth linear dependence for PMMA**

were evaluated and depicted into the graphs. Approximating straight-line and their correlation coefficients were created for these dependencies.

Because of exact evaluation of machined groove profile cuts of specimen were made and then these ones were grinded. This exploration was realized on the optical microscope MU ZEISS. Suitable microscope optics which ensured 250 x enlargements was set first of all. Than digital camera was installed in microscope and it scanned photo of specimens. Photos of grooves and melted boundaries were made. (Fig. 3).You can see the photo of groove detail ABS, PMMA on the following picture.

Digital photos were modified with the help of software ADOBE PHOTOSHOP 6.0 and AUTOCAD 2002. Scales factor corresponding used optics of microscope were assigned at modified photos. Modified photos in JPG format were imported into software AUTOCAD 2002 for the purpose of profile groove digitalization of cut. Lower left corner was localised into coordinate global basic origin. Profile groove of cut was digitized by 30 pixels at coordinates [x, y]. These coordinates were multiplied by corresponding scale so that value corresponded to real values in mm (bitmap inserts into AUTOCAD 2002 is not in real scale). Subsequently the model was defined with the help of software DataFit V.8 :

$$h = A + B.e^{-(x-C)^2} \qquad (1)$$

and numerical values of coefficients A, B, C were itemized. Finally nonlinear regression was realized with the help of DATAFIT V.8. Results of these tests are presented thereinafter on the following figures.

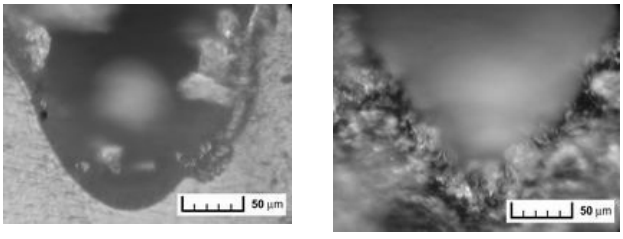

Fig. 3. **The illustration of groove 50/10 ABS and PMMA**

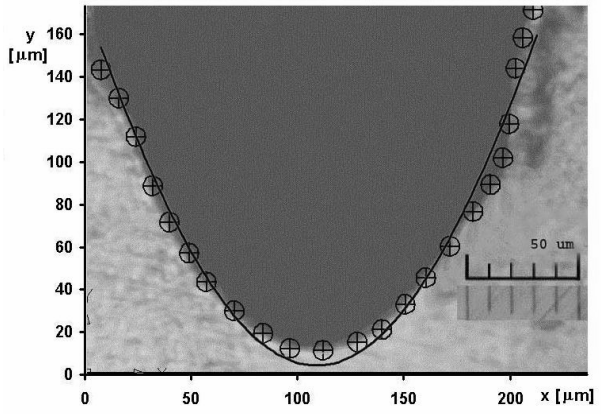

Fig. 4. **Gaussian density of laser beam energy for cutting parameters 50/10, material ABS**

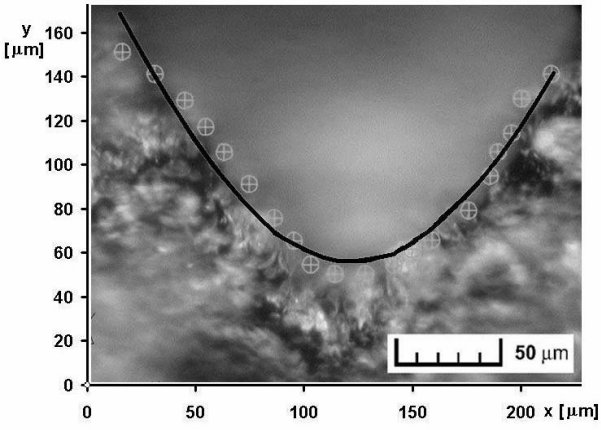

Fig. 5. **Gaussian density of laser beam energy for cutting parameters 50/10, material PMMA**

Conclusions and intentions

From this experiment it is evident the slot depth grows linear with increasing values of power at concrete adjusted value of feed. Biggest depth is at low values of feed. This phenomenon was observed at all materials. Biggest slot dept vas measured at PMMA material. Gradient of lines and corre-

lation coefficients offer information about dependence character of slot depth on adjusted power and feed at graphic presenting results. Value of gradient (k) is used for exact control of stock removal (slot depth). Gradient of line gives information about sloth depth at increasing of power about definite number of percents. Correlation coefficient gives approximate quality of linear dependence (compare with $R^2 = 1$).

Resulting structures can be very exact and with high quality of surface in dependence on laser parameters and on type of machining materials.

From results of experiment is evident that density distribution of used laser beam is Gaussian. The TEM $_{00}$ mode is ideal for most cutting, drilling, and welding applications because it produces a beam that can be focussed to a minimum spot size for very high power density. It is a Gaussian mode, with most of the energy in the centre.

This work was supported by the Ministry of Education and Youth of the Czech Republic under grant MSM 7088352102. This support is very gratefully acknowledged.

REFERENCES

1. Bílek O., Lukovics I. (2006). Manufacturing Technology, J. for Science, Res. and Production. December 2006, vol VI, Ústí nad Labem, p. 12–16.
2. Lukovics I., Bílek, O. In.: Acta Mechanica Slovaca, Košice, 2B/2006, Pro-tech-ma, ročník 10, Košice 2006.

P-45
RESEARCH OF THE LASER TECHNOLOGY

LIBUŠE SÝKOROVÁ and OLDŘICH ŠUBA

Tomas Bata University in Zlín, Faculty of Technology, Department of Production Engineering, T. G. Masaryka 275, 762 72 Zlín, Czech Republic
sykorova@ft.utb.cz

Abstract

The paper deals with possibilities of using the laser in technologies. It evaluates the influence of design and technological conditions on output parameters of cutting process, and also presents relative laser workability of some polymers. Finite element analyses of the transient nonlinear heat and mass transfer were simulated using of the two-dimensional model.

Introduction

The term „laser“ tells us that a simplified description of the lasing process could be „opposite of absorption”. At the heart of the lasing phenomenon is the ability of photons to stimulate the emission of other photons, each having the same wavelength and direction of travel as the original.

The photons oscillating from one end of the resonator to the other constitute electromagnetic energy which forms an intense electromagnetic field. The shape of this field is critically dependent not only on the photon wavelength, but also on the mirror alignment, curvature, and spacing, and on the bore diameter of the laser tube. This field can assume many different cross-sectional shapes, termed transverse electromagnetic modes (TEM), but only certain modes, or mixtures of them, are useful for processing materials. The TEM 00 mode is ideal for most cutting, drilling, and welding applications because it produces a beam that can be focussed to a minimum spot size for very high power density. It is a Gaussian mode, with most of the energy in the centre.

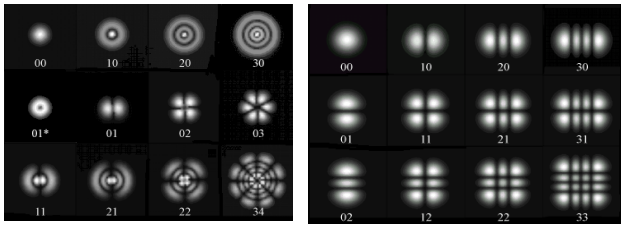

Fig. 1. **Selected Mode TEM**

This mode distributes the beam energy efficiently for other heat-treating and drilling applications. TEM01 also has its particular uses. But not the difference between the cross-sectional representation of the widely used TEM00 mode and that of mode called TEM11.It is evident that the distribution of power across the TEM00 beam, results in a more efficient tool for cutting than does the more fragmented power distribution of the divided TEM11.

Experiment

Absorption of luminous radiation and followed heating depend on thermal conductivity of material. Heat convection from the laser to the material is complicated effect. Today true theory for formulation of thermal conductivity and temperature calculation isn´t exist because heat transfer is very quick. The process propounded by Carslaw-Jaeger is used for formulation of heat transfer for mobile source with speed in (m s^{-1}). The process presents solution partial differential equation for heat convection from the source with dimension of focused beam to surface layer and in material at definite marginal conditions. It goes from simplified hypothesis that material of product is isotropic and heat transfer can describe by Fourier-Kirchhoff differential equation:

$$\frac{\partial T}{\partial t} = \alpha \nabla^2 T \quad , \qquad \alpha = \frac{\lambda}{\rho c} \tag{1}$$

where λ is thermal conductivity, ρ is density, c is heat capacity.

A PMMA side wall gradually cools after a laser light passed through in a specific cut. At the same time, the thermal flow is distributed from a cut plane to the internal dimension of the wall. Thermal conductivity of thermoplastic materials is (100–1000) times less then that of metals. As a result, plastics keep high differences of temperatures between external and internal layers. The physical characteristics of the thermo-

plastic materials were changed significantly in this temperature interval. Values λ, ρ, c were entered as the function of the temperature through the medium of the thermal curves. The heat flow values were entered as the variable parameters. Progressive ignition and extinction of the heat flow simulates the ray laser movement. The maximal temperature was regulated on the already alluded cracking temperature by repeated changes of the heat field value and following thermal field calculation. The time variable heat flow was entered into the particular flat elements (constituent the model half of cut) by time curves i=1,2,3. (Fig. 1).

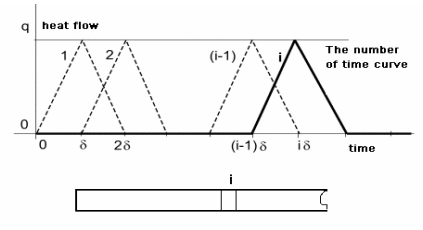

Fig. 2. **Scheme of boundary conditions of the movement ray laser**

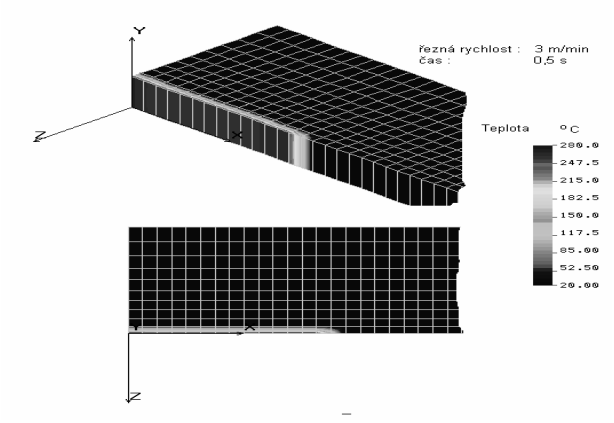

Fig. 3. **The thermal field for cutting speed $1{,}6\times10^{-3}$ ms^{-1} in time t=15 second**

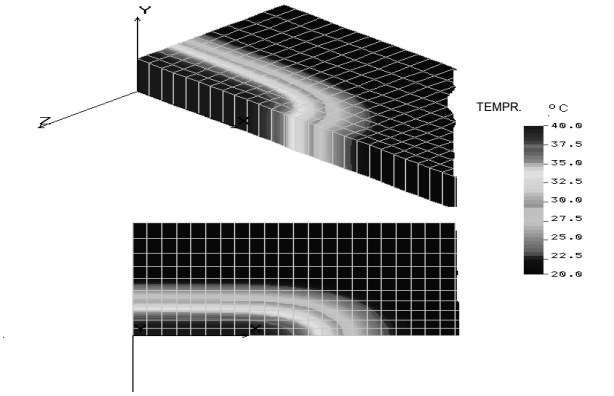

Fig. 4. **Simulation of the heat distribute at surrounds after 3 min**

The results are presented in the following pictures.

Defining and determining of laser workability is a big problem. More workplace for laser cutting determines possessiveness that 15 input variables, further on by time and space variable physically − mechanical and chemical properties of machined material, scoria and the fact, that during the cutting plasma arises. According to our experience it is the most advantageous to define the laser workability with the help of isometric h-v of P-v diagrams. They are describes dependence between depth of cut (h) on laser cutting speed for some metals for range of power (P). Dependencies of laser cutting speed on power for some materials are shown in Fig. 5. Relative laser workability has been defined. It is characterized with the depth of the depth of the cut related to the unit width of the cut and unit output.

The results of the experiments so show very good relative workability of materials and composites whose particles do not tend so separate during the process. If technological conditions (moving speed of the laser head, the beam output, mode parameters of the optics) are optimized, a good quality of the cut can be reached for both metals and plastics.

In case of polymers (plastics and rubber), the surface modification is completely different. During exposition of polymeric material (PP, PS, PE, PC, PVC, PA) samples to concentrated energy, the surface layer degrades and the strength of the samples derogate. On the other hand, PMMA and metal are influenced in a different way. When the output (and therefore heat) increases, the metal material surface is heated above modification temperature. It causes structural transformations in surface layer. The result is a hardened surface layer of the metal and improved strength of samples.

The effect of the laser beam upon PMMA is of interest, too. Due to the layer structure modifications, the surface hardness rises, flaws and creases are healed and as the result of this the sample strength increases. Due to the activity of high concentrate energy and at the same the high temperature, PMMA depolymerize and it rise an amount of radicals at the end of the polymer strings. Thanks to existing of radicals and minor amount of monomer, it raises a net structure here and so the layer strength increases. The strength of the machined layer depends on the time of interaction, too. Longer time of the laser beam contact to material imports better material

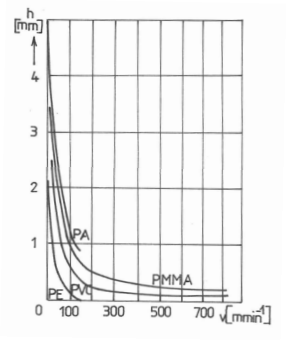

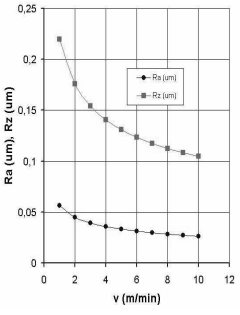

Fig. 5. **Results of laser cutting for some polymers**

strength and hardness. This phenomenon is typical for plastics and it can be useful in special tools manufacturing.

Conclusion

Laser beam is the tool of the future. It can cut without affecting the surrounding material. Its energy is clean, reliable and docile it's ready to be tamed and handled to give an unequalled quality to the process. Quality of cut depends from working parameters of laser cutting process (laser power, feed rate, material thickness.)

The results of the experiments so show very good relative workability of materials and composites whose particles do not tend so separate during the process. If technological conditions (moving speed of the laser head, the beam output, mode parameters of the optics) are optimized, a good quality of the cut can be reached for both metals and plastics.

The model LASER interaction with thermoplastic material is possible. The result area of the high temperature respectively its gradients are narrow after passing of through the LASER ray. The width of the thermal influence area is only a minimal depends on the cutting speed. The high temperature gradients induce both short time transient thermal stress values and residual tension at the cut proximity.

This work was supported by the Ministry of Education and Youth of the Czech Republic under grant MSM 7088352102. This support is very gratefully acknowledged.

REFERENCES

1. Lukovics I., Sýkorová L.: In.: WORKSHOP 97., 1996, p. 1433.
2. Varga V., Maňková I.: In.: Technologia 95 STU Bratislava, 1995.
3. Bílek O., Malachová M.: Academic Journal of Manufacturing Engineering. Politehnica University of Timisoara. 2007, no. 3, s. 16–20.
4. Mádl J., Jersák J., Holešovský F.: *Jakost obráběných povrchů.* UJEP, Ústí nad Labem 2003.

P-46
INFLUENCE OF TENSIDES ON PROPERTIES OF RUBBER BLENDS

MARTINA ŠARLAJOVÁ[a], PAVOL ALEXY[a], JANKA JURČIOVÁ[b], PETER POČAROVSKÝ[a], and JANA ĎURFÍNOVÁ[a]

[a] STU Bratislava, [b] Saar Gummi Slovakia, Dolné Vestenice, Slovakia
martina.sarlajova@stuba.sk, pavol.alexy@stuba.sk, jana.jurciova@saargummi.com, peter.pocarovsky@stuba.sk, jana.durfinova@stuba.sk

Introduction

Tensides are substances which are able to decrease the surface tension on interfaces. Tensides are utilised in polymer blend preparation process for modification of interface between polymeric matrix and particles of inorganic filler. They improve compatibility of polymeric matrix (usually with lower polarity) with surface of more polar filler. Simultaneously addition of tensides causes better properties of blends as an affect of better dispergation of filler in the matrix. Active and inactive fillers have significant influence on properties of vulcanisates. High degree of distribution and high degree of dispergation are necessary to achieve the optimal properties of filed vulcanisates.

In the present work, the influence of two types of tensides (Triton X 405, Tween 40) on properties of rubber blends was tested. Rubber blends based on natural rubber were used in combination with two types of fillers – silica (Perkasil KS 408 PD) and clay (clay KKA). Tensides were dosed at five concentration level from 0 to 5 phr. Influence of type of tenside as well as influence of its concentration on vulcanization parameters and mechanical properties were tested. Morphology of blends was observed using scanning electron microscopy (SEM). Fracture surfaces were prepared by breaking of samples at liquid nitrogen temperature.

Materials and methods

Two types of tensides were used in the work – Triton X 405 (nonionic tenside, octylphenol ethoxylate from Procter&Gamble) and Tween 40 (polyoxyethylen sorbitan monopalomitate from Procter&Gamble). Two types of filler were used as well – Perkasil KS 408 as silica from Werba-Chem GmbH Wien and clay from LB Minerals s r. o. Horní Bříza. Natural rubber SIR 10 was used as rubber matrix. Vulcanisation system consisted from sulphur, ZnO and strearic acid. Sulfenax CBS (sulphenamide) and diphenylguanidine were used as accelerators. All components of vulcanisation system were dosed at 4,5 phr. Paramo MES (mixture of residual and refined oil) was used as well. All mixtures were prepared using brabender chamber kneader, volume 75 ml. Cline loading was 10 kg. Blends were prepared in two stages. In the first stage rubber, oil, filler, tenside, ZnO and stearic acid was blended together during 9 minutes 30 seconds. Temperature of first stage was 90 °C and rotor speed was 50 rpm. Temperature in second stage was 80 °C, rotor speed was 50 rpm. Sulphur and accelerators were blended in this stage during 6 minutes. Final blend was calenderd on calender. Vulcanisation curves were measured at 150 °C using Rheometer Monsanto R100. Vulcanisation parameters were calculated based on recorded vulcanisation curves. Optimum of vulcanisatiom (t_{90}), torque increment (ΔM) and scorch time (t_{02}) were evaluated. Plates with dimension 150x150x2mm were pressed at temperature 150 °C and time of vulcanisation was according to optimum of vulcanisation. Tensile test according to standard ISO 37 was done and tensile strength at break as well as elongation at break were evaluated. Fracture surfaces of vulcanisates were prepared under liquid nitrogen for SEM measurements. Tesla BS 300 with Tescan interface was used for scanning electron microscopy. Relative values of measured properties were calculated for more objective evaluation and comparison of obtained results. Relative values were calculated according to the next formula:

$$P_{rel} = \frac{P}{P_0} - 1$$

where P_{rel} are relative properties, P are measured properties at given concentration of additive and P_0 are properties at zero concentration of additive. All graphs are drawn for relative values of measured properties.

Results and discussion

Both tensides were dosed into blends in concentration 1, 2, 3 and 5 phr while filler content was kept at constant concentration 40 phr. Filler free compounds were prepared for both tensides as well.

Tensides causes decreasing of t_{90} approx. about 20–25 % calculated from its value for blend without tensides (Fig. 1).

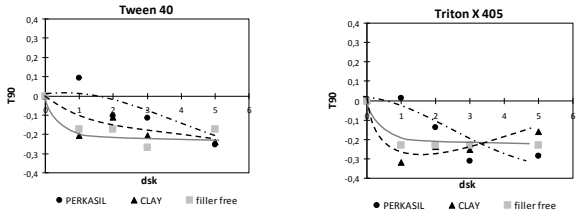

Fig. 1. **Dependency of t_{90} on concentration of tensides**

Decreasing is significant only after addition of 1 % of tensides. No other changes were observed above this concentration in case of filler free blends. Dependencies are slightly different if fillers are applied. In both cases t_{90} decrease, but at lower concentration of tensides decreasing of t_{90} is stronger in case of clay. At higher concentration of tensides decreasing of t_{90} is similar for both fillers.

Mechanical properties of prepared vulcanisates are representing by tensile strength at break (TSb) and elongation at break (Eb). Dependencies of these parameters on type and concentration of tenside are shown on Fig. 2 and 3. TSb slightly decreases (about 5–10 %) if only Triton X 405 is used at concentration up to 5 phr without fillers. In the opposite, if fillers are applied, TSb increases. Increasing of TSb in case of silica is more intensive (up to 15 %) in comparison to clay (up

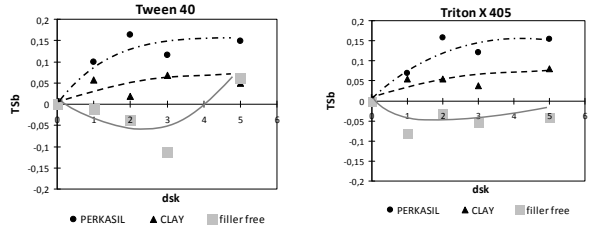

Fig. 2. **Dependency of TSb on concentration of tensides**

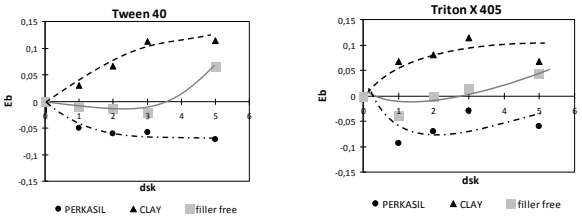

Fig. 3. **Dependency of Eb on concentration of tensides**

to 5 % only). Similar effect can be observed also in case of Tween 40 except dependency of TSb if only tenside was dosing. In such case TSb after very small decreasing significantly increase if concentration of Tween 40 is higher than 3 phr but this effect have no influence on dependency of TSb in case of filled blends.

Elongation at break (Eb) for both tested tensides exhibit practically no changes if tensides are used in unfilled blend up to 3 phr. Above this concentration of tensides Eb slightly increase (approx. up to 5 %). Effect of concentration of tensides on Eb is different for both fillers. Eb significantly increases if clay is used as filler and decreases in case of silica. Increasing respectively decreasing level is approximately the same for both types of tensides.

Based on results obtained from evaluation of mechanical properties, it can be said that applied tensides have positive effect on TSb. Application of tested tensides causes increasing of TSb for both fillers. Effect of tensides is higher in case of silica in comparison to clay. Eb increase or decrease with concentration of tenside in dependency on type of filler. Silica exhibit decreasing and clay exhibit increasing of Eb in dependency on tenside concentration.

Effect of tensides on morphology of vulcanisates was studied using the SEM method. SEM pictures of fracture surfaces are shown in Fig. 4. Differences in dispergation can be observed on SEM pictures in dependency on type of tenside as well as on type of filler. The pictures for blends without filler were done for background identification. Fracture surface shows relative good dispergation of Perkasil particles for both tested tensides. Agglomerates with dimension from approx. 100 nm up to approx. 1–2 μm can be observed on fracture surface for both types of tensides. This results can confirm that both types of tensides improve the dispergation ability of silica, but also it have to be said that the distributive part of mixing proces was not sufficient because described agglomerates create relatively large domains in rubber matrix. This effect is probably caused by insufficient homogenisation ability od Brabender laboratory kneader and the better distribution can be expected if industrial kneader will be used.

The different ability of tensides to satisfy dispergation of filler was observed if clay was used as filler. Better dispergation was observed if Tween 40 was applied. Clay was dispersed in this case into parts with thickness from approx. 400 nm to 700 nm and with longitude up to approx. 10 μm. Triton X 405 gives bigger domains of Clay with dimension in range of microns.

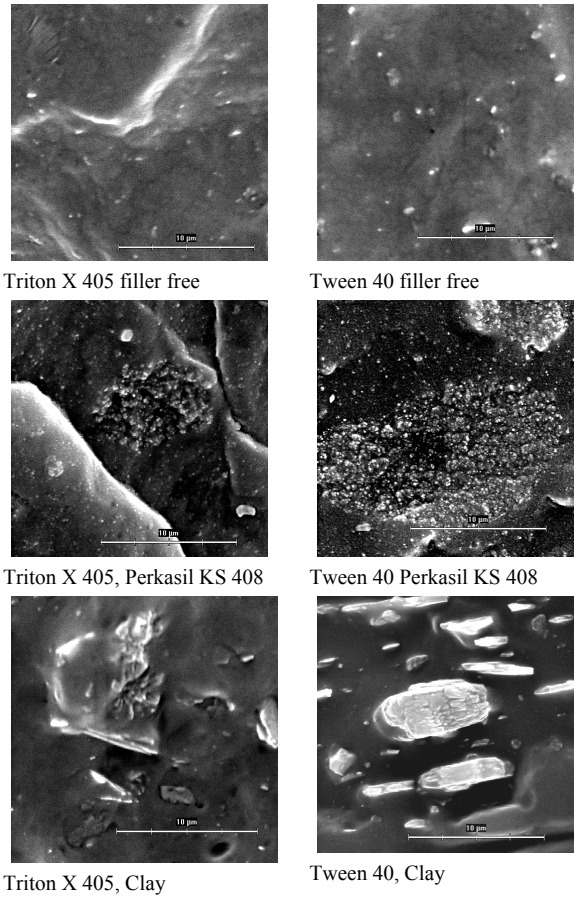

Fig. 4. **SEM pictures of fracture surfaces for samples with 5 phr of tenside**

Conclusion

Results presented in our work show that tested tensides have the significant influence on morphology of final vulcanisates as well as on mechanical properties and vulcanisation parameters of rubber blends. Effect of both tensides is similar if silica is used as filler, but in case of clay Tween shows better dispergation ability in comparison to Triton. Improvement in mechanical properties due to better dispergation of fillers was at level from 5 to 15 %. The higher improvement can be expected if industrial blender will be applied because of better homogenisation and dispergation ability in comparison to laboratory kneader.

REFERENCE

1. Blažej A., a kol.: *Tensidy*, ALFA, Bratislava 1977.

P-47
APPLICATION OF INTEGRATED TEXTILES IN THE AUTOMOTIVE INDUSTRY

KATARÍNA ŠČASNÍKOVÁ[a], JARMILA BALOGOVÁ[b], MARTIN JAMBRICH[c], JAROSLAV LUČIVJANSKÝ[b], and KATARÍNA ŠTEFÁNKOVÁ[c]

[a]Faculty of Chemical and Food Technology, STU Bratislava, [b] Chemosvit – Fibrochem, a.s. Svit, [c] Faculty of Industrial Technologies Púchov, Trenčín, University Alexander Dubček, Slovakia
scasnikova@tnuni.sk

Abstract

This paper deals with the preparation, structure and properties of integrated textiles from the mixture special of polypropylene (PP), elastane (El), polylactide (PLA), bamboo (Bs) and cotton (ba) fibres. The used fibres for the preparation of integrated textiles – fibrous materials, which are introducing raw base of synthetic, microbial and celullose polymers. These fibres are from conventional and from renewable sources of raw materials. Fibrous materials – textiles based on mentioned types fibres having good physiological, physical-mechanical and with wide scale utility properties.

Introduction

Current development fibers is directed towards the preparation new or innovative materials in all branches of industry. The main requirement is that these materials solely high user demand and were also environmentally friendly, ie readily biodegradable and recyclable[1,3]. The essence of the solutions which solely these trends are well integrated fibrous materials for clothing, furnishing and technical textiles on the basis of renewable fibers from biodegradable polymers and synthetic fibers[2].

Integrated fibrous materials prepared in the form of knits and woven fabrics usually contain structurally different types of chmical fibers from renewable, biodegradable, compatible and antimicrobial materials (bamboo, polylactide, cellulose) and synthetic fibers (polypropylene, elastane), or mixtures thereof in admixture with at least one auxiliary material[2].

Much attention has been devoted to preparing many-component fibers and fibrous materials for integrated textiles, mainly to increase physical activity. One approach to increase utility properties fibers is a modification of the transverse and longitudinal geometry fiber, but also change the surface properties of fiber by physical modification of suitable additives such as increasing. hydrophilicity of the material. Selection and application of appropriate modification process to improve the properties of PP fibers depends primarily on the requirements that are imposed on their use[4,5]. Modifications of polymer additives, nanoparticles, dendrimers, branched polymer, and polymers for the preparation of polymer blends counts among the most studied modifications to improve the properties of fibers in recent years[6]. Modifications of the PP fibers are primarily directed at the increasing hydrophilicity

PP. Among the modifications that have been studied at improving hydrophilicity PP fibers we can include: esc. grafting of a PP membrane surface with poly(*N*-vinyl-2-pyrrolidone) and PP hollow fibers membrane surface with *N*,*N*-dimetylaminoethyl metacrylate leads to the higher hydrophilicity of a PP surface[7].

Theme of our work is focused on preparation of integrated fabric of PP fibers 56/33x2 with a hydrophilic additive, PP 56/33x2 and PP 56/43x2 from hollow fibers that are combined together with El, PLA and Bs fibers. Creating space for expansion of knowledge in this area particularly in relation fiber type, its structure and utility properties of the product. This article is focused on the preparation and evaluation of physico-chemical, physiological and utility properties of integrated textiles – knitted fabrics with different composition of the fibers used.

Theoretical part

Preparation commercial types polypropylene fibers is based on the use of isotactic polymer chirality. The new generation of m-iPP polymers can be prepared fibers with lower weight and higher measuring physical – mechanical properties. Metallocene PP types of polymers are the real basis for qualitative progress in the assortment of PP fibers. Macromolecular chain iPP is characterized by recurring monomer unit. In fact, the influence of bulky isotactic chain – CH3 groups interested in a regular conformation (gauche), which is reflected in good crystallizable polymer, in its strength and stiffness. The only intermolecular forces are Van der Waals[8,9].

Polyurethane fibers are made of glycol and diisocyanate special spinning method. These fibers can also be manufactured from hexamethylene diisocyanate, but have less meaning[10].

Cotton fibers are the natural cellulose fibers, which is a constituent of cellulose fibers of plant origin. Macromolecules in the form of cellulose fiber axis elementary fibrils, which are linked to senior staff, protofibrils and microfibre, and these aggregate into fibrils. Layers of fibrils form lamellae, which form the cell walls of fiber[11].

Bamboo fiber belongs to the cellulose fibers of regenerated cellulose, which is made from bamboo pulp prepared from bamboo plants. Bamboo pulp is extracted from the bamboo and the process of hydrolysis alkalization and multi-phase bleaching. Process for the preparation of bamboo fibers is similar to the preparation process of viscose fibers. Bamboo is a typical natural composite material, which is the length reinforced by strong fibers. Fibers are densely distributed in the outer surface area and sparsely in the inner part. Bamboo fiber is biodegradable in soil microorganisms and sunlight. Folding process does not cause any pollution environment. This thread is considered natural and EKO – acceptable type of textile material[12].

Polylactide fibers are assigned to groups of microbial chemical fiber types. The favorable development of microbial polymers is due to the limited resources of fossil raw materials. Polylactides are produced from lactic acid. Fibers from polylactic acid are biodegradable and biokompaktibilný type, which represents the character of its properties of natural and synthetic fibers. PLA fibers are a new kind of biodegradable and biocompatible fiber type available source material. Properties of PLA fibers and renewable resource materials predispose them to be future fiber[4,12].

Experimental part

Our experimental work focused on the preparation of integrated fabric – knit of hydrophobic and hydrophilic fibers and evaluation of their structure, physico – mechanical, physiological andutility properties. The following types of fibres were selected for the preparation of integrated fibrous materials:

- polypropylene fibres with changed reluctant geometry (hollow) as hydrophobic unbiodegradable type,
- polypropylene fibres without changing reluctant geometry (full) as hydrophobic unbiodegradable type,
- polypropylene fibres with using of hydrophilic additive, unbiodegradable type,
- synthetic, hydrophobic, unbiodegradable elastane fibres,
- cellulose, hydrophilic, biodegradable type from the renewable resources of raw materials (bamboo) with antibacterial efficacy,
- cellulose, hydrophilic, biodegradable type – natural fibre – cotton,
- polyactid (PLA) – microbial, hydrophobic and biodegradable type with the changed reluctant geometry (hollow) from renewable resources of raw materials.

For fibers and yarns were evaluated:

- Physico-mechanical properties (determination of linear weights (fineness) fibers, fiber strength and elongation, the number of seats previre (PPM), the number of fibrils and the determination of fibers contraction (KK – value)).
- Evaluation parameters and structure of the fibers – yarns (transverse and longitudinal evaluation of the geometry of fibers, microscopic method, determine the speed of sound propagation in fibers, melting, crystallization and crystalline fibers share)

For fabric:

- Macromorfological structure and geometric properties.
- Physico – mechanical properties (determination of strength, ductility printed textiles, fabric areal weight).
- Physiological properties (determination of sorption, wetting contact angle, thermal – insulation thermocontact method for device ALAMBETA).

REFERENCES

1. Dirk De Saedeleir, Alain Goossens, The U.S. Manufactured Fiber and Textile Industry : Innovative applications of biopolymers, *48th International Man-Made Fibres Congress, Dornbirn, 16-18 September 2009*, Austria.
2. Jambrich M., Macho V., Olšovský M., Balogová J., Vnenčáková J., Sroková I., Benčíková E.: Vláknité materiály na ošatenie a/alebo bytové textílie. Úžitkový vzor - 5182, udelil Úrad priemyselného vlastníctva SR, Banská Bystrica 2.4. 2009.
Herben, P.-Lonardo, A.: Chemical Fibers International *59*, 125 (2009).

4. Jambrich M.: In.: Prednáška na medzinárodnej konferencii *59. Zjazd chemických spoločností, 2.-6. 9. 2007, Vysoké Tatry*.
5. Bolhová E., Ujhelyiová A., Marcinčin A.: Vlákna a textil *11*, 147 (2004).
6. Ujhelyiová A., Bolhová E., Vaľková K., Marcinčin A.: Vlákna a textil *12*, 48 (2005).
7. Krištifič M., Náčiniaková Z., Legéň J., Ryba J.: Vlákna a textil *12*, 104 (2005).
8. Michlík P., Brejka O., Ujhelyiová A., Vnenčáková J. : *7 th International conference Advantes in plastics technology, november 13.-15. 2007 Katovice*, PL, Conference Papers No. 5.
9. Jambrich M., Pikler A., Diačik I.: *Fyzika vlákien*. Alfa, Bratislava 1987.
10. Strecký J.: *Odevné tovaroznalectvo*. Alfa, Bratislava 1996.
11. Jambrich M.: *Chemické technológie celulózových vlákien*. študijný materiál FPT TnU AD, Púchov 2005
12. Ščasníkova K., Balogová J., Benčíková E., Jambrich M., Lučivjanský J., Vnenčáková J.: In: *Prednáška na konferencii TEXCO, Ružomberok, 2010.*

P-48
MODELLING OF TRANSIENT THERMAL STRESS IN POLYMER LAYERED WALLS

OLDŘICH ŠUBA and LIBUŠE SÝKOROVÁ

Tomas Bata University in Zlín, Faculty of Technology, Department of Production Engineering, T. G. Masaryka 275, 762 72 Zlín, Czech Republik
suba@ft.utb.cz

Abstract

Results of FEM modelling of transient thermal stress analysis in layered walls are given in the article. It is shown that thermal stress alone is not solely caused by differences in coefficients of thermal expansion of individual layers. The emergence of transient thermal stress is subject to both the layered structure of the wall and given boundary conditions, as well as the existence of a temperature gradient in the direction normal to the surface of the wall.

Transient thermal stress due to the temperature gradient

Now consider generally layered wall, i.e. a wall with generally varying properties along its thickness, exposed to thermal effects with random thermal profile ΔT(y) corresponding to a certain moment of transient heat transfer through the wall – Fig. 1.

Not only the elastic constants but also the coefficient of linear thermal expansion generally changes both discontinuously at the layer interface and continuously within each layer due to possible dependences of constants on temperature.

This task can be seen as a wall imaginary composed of an infinite number of layers of elementary thickness dy; each layer has its own values of elastic constants and thermal expansion coefficient. The value ΔT(y) expresses the difference between the real temperature at place y and the reference temperature of the wall, i.e. temperature at which zero stress of the wall is assumed.

Let the wall be gripped again in a way which prevents its warpage but allows membrane deformations, i.e. deformations in the directions of the reference surface are possible. The resulting membrane forces in the wall sections then equal to zero, so that

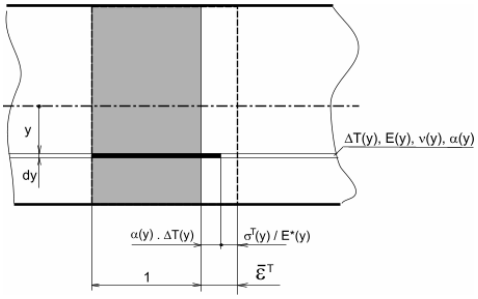

Fig. 1. **Generally layered wall**

$$\int_{(s)} \sigma^T(y)dy = 0. \qquad (1)$$

Unless there is warpage of the wall, the sum of thermal expansion and elastic deformation, which is in each imaginary layer dy constant, equals to ε^T. Considering that this is an equibiaxial stress, so that

$$\varepsilon^T = \frac{\sigma^T(y)}{E^*(y)} + \alpha(y)\,\Delta T(y) \qquad (2)$$

When using (*1*), the final uniaxial wall deformation can be expressed by the following relation

$$\varepsilon^T = \frac{\int_{(s)} E^*(y)\;\alpha(y)\;\Delta T(y)\;dy}{\int_{(s)} E^*(y)\;dy}. \qquad (3)$$

Thus equibiaxial stress in the area of ordinate y will be

$$\sigma^T(y) = E^*(y)\left[\varepsilon^T - \alpha(y)\,\Delta T(y)\right]. \qquad (4)$$

The expression (*4*) does not apply in areas of free edges of the double-layer wall, where the boundary stress-tops form, especially those of shear stress components at the layers interface. Tension given by the relation (*4*) is transient (time dependent) in cases of time-variable temperature field. After disappearance of the temperature gradient, stress also disappears.

FEM modelling of transient thermal stress

In recent years the development of consumer electronics has brought the necessity of electrical waste recycling due to falling prices of electronics, and thus its massive consumption, and also a decrease of its lifetime[1].

Although the formation of thermal stress can be generally regarded as a negative phenomenon in terms of utility properties of plastic and composite products, in practice there are cases in which thermal stress is formed deliberately. This is the case of PCB boards recycling; the aim is to break the interface and thus separate individual layers with the use of thermal stress. The role of thermal stress modelling in this area lies in predicting the possibility of separation in dependence on the type of thermal stress and material parameters of the layers.

FEM modelling of transient thermal stress states runs in two stages. Firstly, the appropriate thermal boundary conditions of the board are set and the instantaneous profiles of the temperature field are calculated in the chosen time steps. Time-variable thermal boundary conditions are entered via so-called time-curves. Secondly, the appropriate mechanical boundary conditions are set and the instantaneous values of transient thermal stress components are calculated for the chosen time frames of the course of the temperature in the board. Whereas the mechanical and thermal parameters of the material layer 1 (Cu) can be considered to be temperature-independent in calculation, the layer of polymer composite 2 shows strong temperature dependences of physical properties on temperature, especially that of the modulus of elasticity.

Therefore these dependencies were generalized by appropriate temperature curves in calculation. Thus the composite layer becomes quasi-layered during pull of the temperature gradient on its thickness; it means that the individual equidistant planes, respectively imaginary layers of elementary thickness, show different values of thermoelastic properties at the given instant of time.

Time curve of the chosen model of thermal process is shown in Fig. 2. The PCB board is heated to the temperature of 200 °C. By the immersion into brine of the temperature of −10 °C the surface is rapidly cooled to this temperature in the time interval of 1–2 seconds. Then the board remains in the bath until the disappearance of the thermal gradient, i.e. until the temperature fully reaches the value of −10 °C.

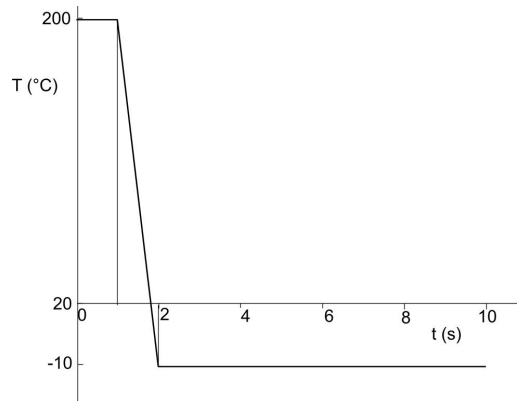

Fig. 2. **Time curve of the temperature on the PCB board surface for modelling of rapid, i.e. non-homogenous, cooling**

Conclusions

After the analysis of the time-variable temperature field the results of chosen time moments are used for the analysis of thermal stress. Values of biaxial normal stress in individual layers according to (*4*) do not themselves affect the separation of the layers. It depends on the existence of peaks of shear components on the edges of layers at their interface directly proportional to normal thermal stress. Type of course of shear stress at the layers interface is shown in Fig. 3. In a certain instant of time stress reaches its maximal value at the edge of the layer 1(Cu). Stress extends in direction from the edge to the distant L_0, which is the same order of magnitude with the thickness of polymer layer (*2*). If the maximal value of shear stress at the interface reaches the limit value – shear strength of interface, the separation begins. The resulting course of time dependence τ_{MAX} from the beginning of the board cooling is shown in Fig. 4. As can be seen, in process of rapid, i.e. non-homogenous, cooling there is the instant of time tmax in which the peak of shear stress reaches its maximal value.

Since the beginning of cooling the values are increasing to this value and after reaching it they decrease to the zero value when the temperatures in the board evened out. The

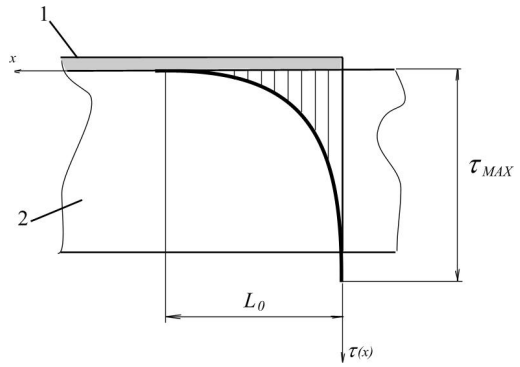

Fig. 3. **Dependence of shear stress at distance x from the edge of the layer 1 (Cu)**

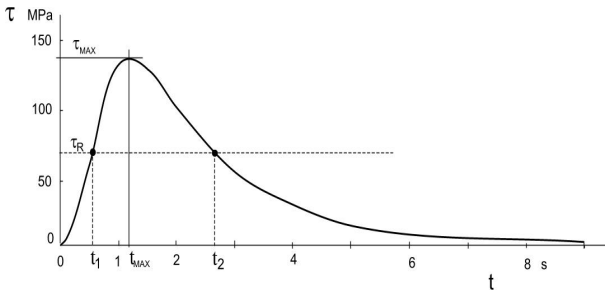

Fig. 4. **Time course of boundary maximal shear stress at the layers interface**

separation process can be characterized as follows: separation begins after rising of τ_{MAX} to the value of shear strength at the interface τ_R – instant of time t_1. The edge of Cu layer starts to peel, whereas the edge of layers joints moves in direction of separation and has a value τ_{MAX} variable in time. The process of peeling of Cu layer stops in time corresponding to decrease of τ_{MAX} to the value τ_R in time t_2.

This work was supported by the Ministry of Education and Youth of the Czech Republic under grant MSM 7088352102.

REFERENCE

1. Janáčová D., Kolomazník K., Vašek V., Mokrejš P.: *The 5th WSEAS Conference on Heat Transfer, Thermal Engineering and Environment HTE'07, Athens, 2007,* 268–271. WSEAS World Science and Engineering Academy and Science 2007.

P-49
EVALUATION OF TENSILE TESTS OF SHORT-FIBRE REINFORCED POLYMERS BY MICROSTRUCTURE FEM MODELLING

OLDŘICH ŠUBA and LIBUŠE SÝKOROVÁ

Tomas Bata University in Zlín, Faculty of Technology, Department of Production Engineering, T. G. Masaryka 275, 762 72 Zlín, Czech Republic
suba@ft.utb.cz

Abstract

The paper gives modelling results of elastic constants dependences on fibre volume ratio and its aspect ratio. 3D totally oriented short-fibre structure is expected. The results are compared with evaluation of stiffness experimental data of injection moulded polymer specimens reinforced with short fibres.

Introduction

Unlike isotropic materials, application of experimental data, obtained in standard tensile tests for the needs of the stress and deformation analysis and practical dimensioning of products made of short-fibre composites is a more complex problem. The result of a standard tensile test is only a value of elastic stiffness in the direction of the sample axis. The injection moulded sample represents, owing to its geometry, a highly oriented structure, which differs as a rule from the structure of products with more complex geometry. It is well known[1] that at higher velocities of the melt stream a „sandwich-type" structure arises. It consists of two surface layers and a central layer – „core". The fibres within both surface layers are oriented almost exclusively in the melt flow direction, while the fibres in the central layer are oriented transversally. Elastic behaviour of the short-fibre composite depends, next to the aspect ratio, on the basic parameter of the short-fibre structure – fibres orientation. In a certain dependence on the degree of orientation, both effective elastic constants and other physical and macroscopic properties are changed. Fibres orientation within the sample is influenced in its different parts by the location of the type of the gate and the shape of the body, or the mould cavity.It is practically impossible to ascertain the set of effective elastic constants of a monotropic- fully oriented short-fibre structure only on the use of experimental measurements. Therefore, a theoretical prediction of elastic constants of the short-fibre composite is very important here. We are presenting experience and results obtained at our department in micromechanics of 3D totally oriented short-fibre structures. These results are then used for the construction of macroscopic module of injection moulded sample stressed by a uniaxial strain. This model is then used to evaluate tensile tests of samples of polymers filled with short fibres.

Modelling of Elastic Constants of Particle Composite with Totally Oriented Fibres

Model structure of the composite with fully oriented short fibres represents a so called representative volume. Individual states of loading of the model volume were processed by means of the FEM software system. Results in a form of dependences of elastic constants of the oriented short fibre structure upon volume concentration of fibres are provided in the following diagrams.

Fig. 1 shows dependence of a longitudinal elasticity modulus in the practical area within the fibres volume ratio 50–100. The result provided in Fig. 2 for the transversal modulus confirms the well- known experience that E_T practically does not depend on fibres volume ratio.

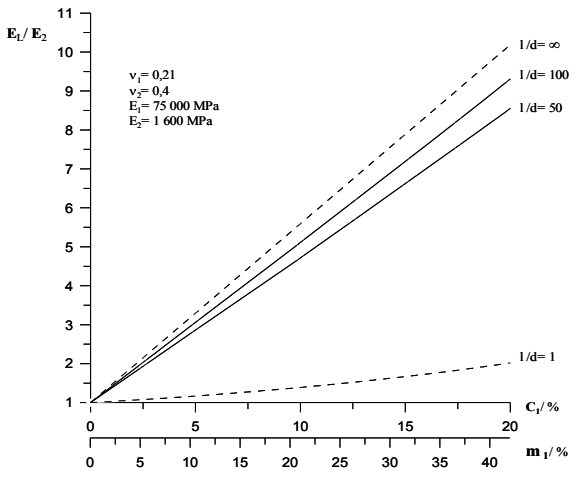

Fig. 1. **Young's modulus in fibres E_L direction in dependence on volume ratio c_1 and aspect ratio *l/d***

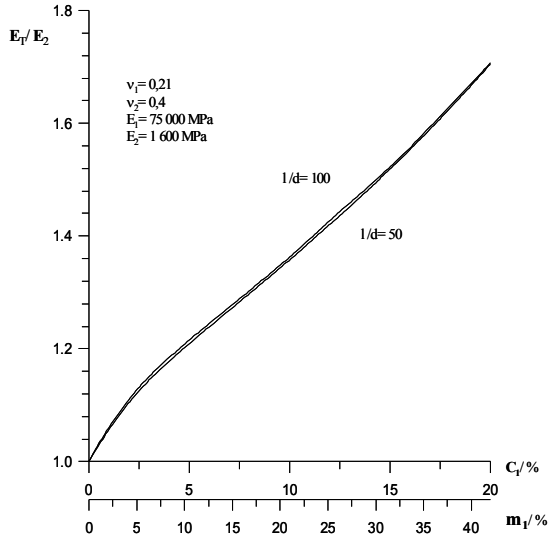

Fig. 2. **Young's modulus in direction transversal to fibres orientation E_L in dependence on volume ratio c_1 and aspect ratio *l/d***

Effective Elastic Constants of Injection Moulded Elements

The values of effective Young's modulus of injection moulded standard testing elements, found out by means of an experiment, were compared with two model imaginations, differing in the assumption of idealization of fibres orientation distribution after the cross-section. In the first case statistically isotropic structure without priority orientation after the cross section area was modelled. This effect was reached by simulation of a higher number of *n* layers, with totally oriented fibres, with a mutual angular displacement π/n. In the second case the relation between the surface layers area (with 0 orientation) and the core (with $\pi/2$ orientation) was supposed to be 2:1.

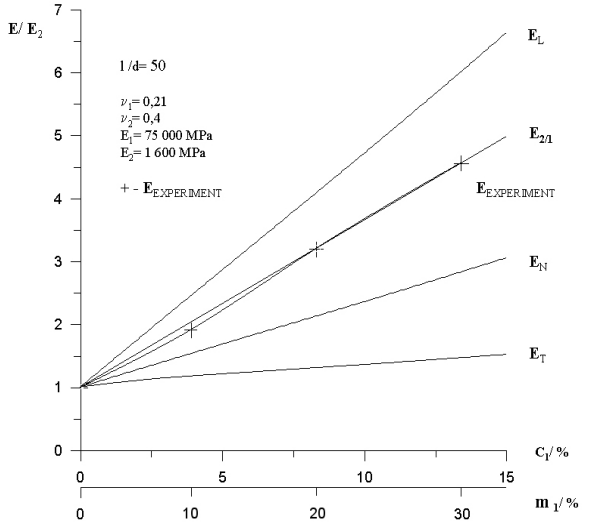

Fig. 3. **Comparison of dependence of effective Young's moduli of model structures with experimental results**

The results are shown in Fig. 3. Experimental data of samples with a different degree of fibres concentration ($E_{EXPERIMENT}$) are compared with theoretical values of the modulus of the totally oriented structure for the longitudinal (E_L) and transversal (E_T) direction, for non-oriented structure (E_N) and layer structure ($E_{2/1}$).

As evident, tensile stiffness found out in experimental measurements approaches the model values of the layer structure the most.

Conclusions

Results of micromechanical and macromechanical modelling of the elastic behaviour of short-fibre composites reached in tests enable to predict elastic behaviour of walls of injection moulded products made on the basis of these materials. In this case the theoretical predictions of elastic constants of short-fibre composite materials were used for determination of an effective Young's modulus in tension at real injection moulded testing products.

This work was supported by the Ministry of Education and Youth of the Czech Republic under grant MSM 7088352102.

REFERENCE

1. Bright P. F.: J. Mat. Sci. *13*, 2497 (1978).

P-50
POLYMER BLENDS OF POLYETHYLENE TEREPHTHALATE AND POLYLACTIC ACID

KATARÍNA TOMANOVÁ, MIROSLAVA PAVLAČKOVÁ, PETER BUGAJ, FRANTIŠEK BENOVIČ, and PAVOL ALEXY

Ústav polymérnych materiálov, Fakulta chemickej a potravinárskej technológie, Slovenská technická univerzita, Radlinského 9, 812 37 Bratislava, Slovak Republic
katarina_tomanova@stuba.sk

Introduction

Polyethylene terephthalate (PET) is a commercially important engineering thermoplastic with good thermal and mechanical properties, low permeability, and chemical resistance. It is used in bottle containers, food packaging, textile fibers, engineering plastics in automobiles, electronics and blood vessel tissue engineering[1]. But it is non-biodegradable and its amount in landfill is still growing, of course, with other synthetic and petroleum-based plastics. A proposed alternative is to develop blends of PET with naturally renewable units like polylactic acid (PLA)[2]. Unlike petroleum-based plastics, PLA is biodegradable green plastic derived from renewable resource, such as starch. PLA is biodegradable polyester with high strength and high modulus. It has

various applications in drug delivery, tissue engineering, food packing and bottle containers. PLA bottles have many advantages such as biodegradability, plentiful material source, and lower processing cost during blow-molding due to its lower glass transition temperature[1]. However, PLA has not good barrier properties and has relatively high cost. Therefore its usage in bottles is still limited. In the present work, mechanical and processing properties of PET/PLA blends were studied. PLA content in the blends gradually changed from 0 % to 100 %wt. Triacetine was used as plasticizer.

Experimental

Materials

- Polylactic acid – PLA 4042D from NatureWorks, LLC, USA
- Polyethylene terephthalate (PET)
- Triacetine as PLA plasticizer

PET/PLA blends preparation

Both polymers PET and PLA were dried 120 minutes at the temperature of 80 °C in hot-air chamber. PET/PLA blends were prepared using twin-screw extruder. PLA content in the blends gradually changed from 0 % to 100 % wt. Thermal profile of extrusion in the direction from feeder to die was set on 250 – 260 – 260 – 260 – 260 – 260 – 255 – 250 – 245 – 240 °C and extrusion speed was 80 rpm. Extruded material was cooled down with cold water and then it was granulated into small pellets.

PET/PLA monofils preparation

Granulated material was dried again 120 minutes at the temperature of 80 °C in hot-air chamber. Dried granules were used to PET/PLA monofils preparation on single-screw extruder, where one – hole die was used. Extrusion speed was 10 rpm.

Measurement of mechanical properties of prepared monofils

Yield strength (σy), tensile strength (σb) and the elongation at break (εb) were measured with Zwick machine at cross-head speed 1 mm/min in the deformation range of 0–3 % and after this value of elongation the speed increased up to 50 mm/min. These properties were determined based on recorded tensile curves.

Results and discussion

At first, monofils from pure PET were prepared at thermal profile 240 – 250 – 270 – 260 °C in the direction from feeder to die. Mechanical properties of prepared PET monofils were measured and Table I shows obtained results.

Also blends PET/PLA with various content of PLA were prepared at the same conditions. Fig. 1–3 show dependencies of tensile strength at yield, tensile strength at break and elongation at break on PLA content in PET/PLA blends.

Table I
Mechanical properties of pure PET monofils

PET [%]	σy [MPa]	σb [MPa]	εb [%]
100	52.61	81.59	919.54

Fig. 1 and 2 show that tensile strength at yield (σy), which is very important property of prepared blends because of their planned application, was minimally decreased at the range of PLA content in blends from 5 to wt.20 % At higher content of PLA in blends, except pure PLA, there was recorded no yield point. Tensile strength at break (σb) of PET/PLA blends was decreased with an addition of PLA nearly to the half.

Fig. 3 shows dependency of elongation at break (εb) on PLA content in PET/PLA blends. Effect of PLA content in blends has already been achieved in its content of 5%. The

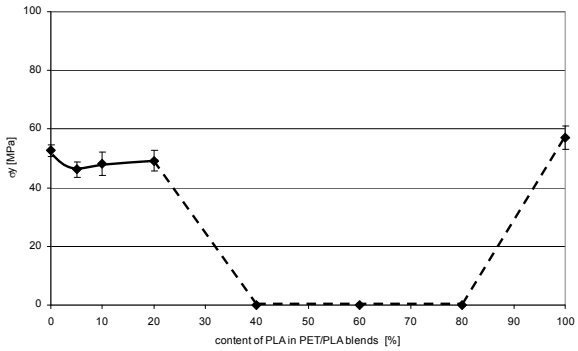

Fig. 1. **Dependence of tensile** strength at yield on PLA content in PET/PLA blends. Zero values of σy mean, that no yield points were observed on tensile curves

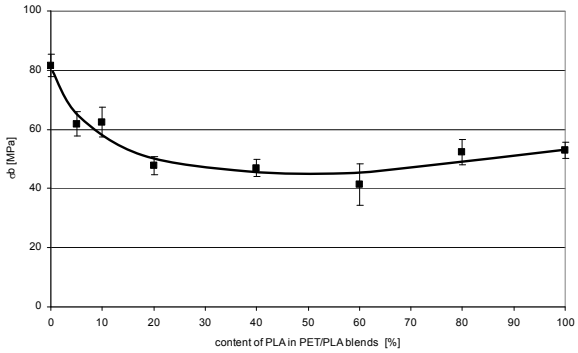

Fig. 2. **Dependence of tensile** strength at break on PLA content in PET/PLA blends

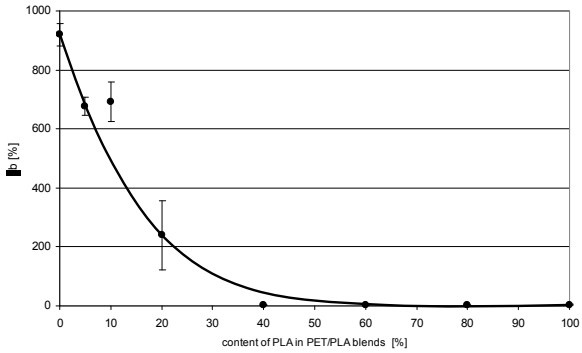

Fig. 3. **Dependence of elongation at** break on PLA content in PET/ PLA blends

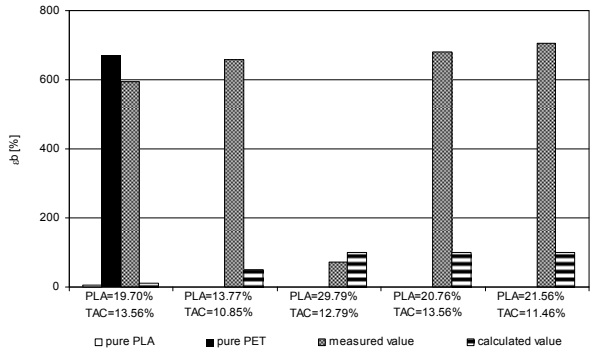

Fig. 6. **Elongation at break** of optimalized PET/PLA blends with various composition

value of εb decreased from 920 % to 3 %. This trend corresponded to elongation of pure PLA.

After research of basic properties of PET/PLA blends, Design of experiment (DoE) method was used in the next part of this work. PLA content in blends varied from 5 to 30 wt.%, triacetine (TAC) was used as PLA plasticizer and its content varied from 6 to 20 wt.%. Thereafter, optimalization of DoE followed. Fig. 4–6 show results of mechanical properties measurements.

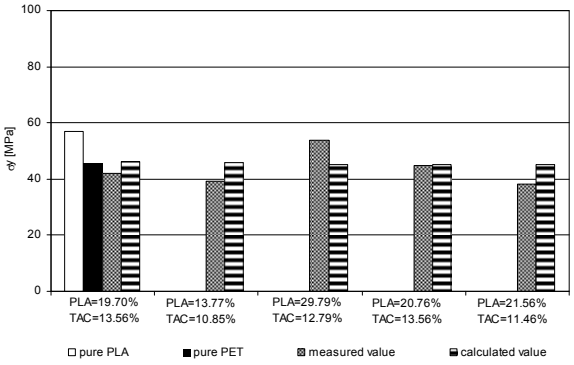

Fig. 4. **Tensile strength at** yield of optimalized PET/PLA blends with various composition

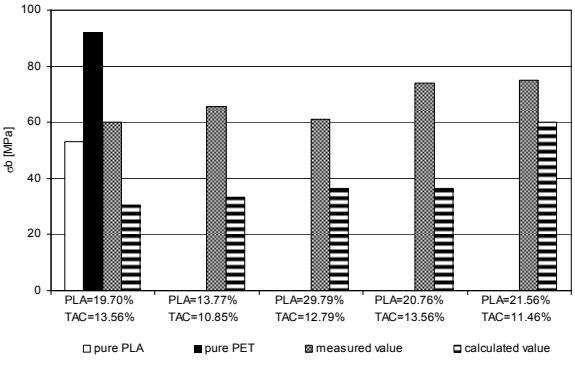

Fig. 5. **Tensile strength at break of optimalized PET/PLA** blends with various composition

Obtained results presented on Fig. 4–6 show coincidence between calculated values and experimental obtained results in case of tensile strength at yield. Worse coincidence can be observed in case of tensile strength at break and the worst one is in case of elongation at break. The differencies between experimental values and values predicted based on mathematical model have origin in relative high regression inadequacy as well as high value of experimental error in case of elongation at break. Nevertheless, experimentally obtained values are much better then calculated values in the most of blends. The positive effect of TAC can be observed mainly in case of elongation at break. Blends containing up to 20 wt.% of PLA reached εb values higher than 600 % in comparison with the blends with same quantity of PLA, but without TAC which exhibit around 200 % of εb. Also tensile strength at break was improved by application of TAC in PET/PLA blends. While TAC free blends of PET/PLA exhibit σb around 50 MPa when PLA content was 20 wt.%, the same blends with TAC reached σb higher than 70 MPa.

Conclusion

Based on reached results it can be concluded that addition of PLA to PET causes significant drop of elongation at break as well as tensile strength at break. This deterioration of mechanical properties can be supressed by addition of TAC as plasticizer. Optimised blends based on DoE results exhibit similar mechanical properties like pure PET up to 20 wt.% of PLA. In the next work processing properties as well as barier properties of PET/PLA/TAC blends will be studied.

This project is supported by Norwegian Financial Mechanism, Financial Mechanism of EEA and State budget of Slovakia – project No. SK 0094.

REFERENCES

1. Huipeng C. H., Pyda M., Cebe P.: Thermochim. Acta 492 (2009).
2. Gipija B. G., Sailaja R. R. N., Madras G.: Polym. Degrad. Stab. 90 (2005).